

Superparamagnetic iron oxide labeling limits the efficacy of rabbit immature dendritic cell vaccination by decreasing their antigen uptake ability in a lysosome-dependent manner

Min Zhang · Jing Zhou · Jingchun Wang ·
Quan Zhou · Jin Fang · Chengqian Zhou ·
WenLi Chen

Received: 13 June 2014 / Accepted: 8 September 2014 / Published online: 26 September 2014
© Springer Science+Business Media Dordrecht 2014

Abstract Immature dendritic cells (iDCs) are for cell transplantation; however, no method has yet been developed for in vivo monitoring the transplanted iDCs. We have explored the feasibility of using superparamagnetic iron oxide (SPIO) labeling and magnetic resonance imaging for in vivo tracking of transplanted iDCs and determined the effects of SPIO labeling on iDC vaccination. With up to 50 µg Fe/ml, SPIO effectively labeled the iDCs without affecting their growth. At or above 100 µg Fe/ml, SPIO caused considerable damage to iDCs. SPIO labeling resulted in autophagosome formation and decreased the uptake of oxidized low density lipoprotein (ox-LDL), an exogenous antigen, by iDCs. SPIO and ox-LDL both localized to the lysosomes, and this competition for lysosomes could be partially responsible for the decreased ox-LDL phagocytic capacity of iDCs due to SPIO labeling.

Keywords Antigen uptake · Autophagy · Cell labeling · Immature dendritic cells · Lysosome · Magnetic resonance imaging · Superparamagnetic iron oxide

Abbreviations

<i>iDC</i>	Immature dendritic cell
<i>DC</i>	Dendritic cell
<i>MRI</i>	Magnetic resonance imaging
<i>SPIO</i>	Superparamagnetic iron oxide
<i>PLL</i>	Poly-L-lysine
<i>FBS</i>	Fetal bovine serum
<i>IL-4</i>	Interleukin-4
<i>GM-CSF</i>	Granulocyte–macrophage colony-stimulating factor
<i>FITC</i>	Fluoresceine isothiocyanate
<i>PE</i>	R-Phycoerythrin
<i>SI</i>	Signal intensity
<i>CCK8</i>	Cell Counting Kit-8
<i>LTR</i>	LysoTracker Red
<i>3-MA</i>	3-Methyladenine
<i>EGFP-LC3</i>	Enhanced-green-fluorescent-protein-tagged microtubule-associated protein 1 light chain 3
<i>DiI</i>	1,1'-dioctadecyl-3,3,3',3'-tetramethylindocarbocyanine perchlorate
<i>ox-LDL</i>	Oxidized low density lipoprotein

M. Zhang · J. Zhou · J. Wang · C. Zhou · W. Chen (✉)
MOE Key Laboratory of Laser Life Science, South China
Normal University, Guangzhou, China
e-mail: Wenlichen511@yahoo.com

Q. Zhou · J. Fang
Medical Imaging Center, The First Affiliated Hospital of
Jinan University, Guangzhou, China

Introduction

Immature dendritic cells (iDCs), which do not or seldom express the requisite accessory signals for T cell activation, can induce immune tolerance (Klotz et al. 2007).

iDCs act as potent immunosuppressors in allotransplantation. The efficiency of iDC vaccines can be improved by varying the optimal dose and route of administration. However, no method has yet been developed for *in vivo* monitoring of the transplanted iDCs. Magnetic resonance imaging (MRI) may provide some answers to these questions (Tavaré et al. 2011). Owing to its deep penetration (from 1 mm to 1 m) and the ability to resolve different soft tissues (Datta and Raymond 2009), MRI in conjunction with contrast agents can be used track transplanted cells (Zhou et al. 2014).

SPIO, an MRI contrast agent, is readily internalized by cells and is relatively stable in the vascular system, thereby allowing extended imaging (Lunov et al. 2010). Moreover, SPIO is biodegradable and clinically approved. Despite high labeling efficiency and low cytotoxicity, SPIO may affect dendritic cell (DC) migration and uptake or antigen processing (Baumjohann et al. 2006). The success of immunotherapy with iDCs for various immune disorders depends on their antigen uptake. However, the effect of SPIO on the antigen uptake ability of iDCs has not been clarified.

In autophagy, long-lived proteins and defective organelles are packaged into autophagosomes and delivered to lysosomes for degradation. Autophagy assists endogenous antigen processing (Jagannath et al. 2009; Paludan et al. 2005) but limited data are available on the effect of autophagy on exogenous antigen processing. Increased autophagy is a widespread phenomenon in cells that have been treated with nanomaterials (Zabirnyk et al. 2007), and SPIO—also a nanomaterial—could presumably act as an autophagy activator.

Herein, we report that SPIO was taken up by iDCs in a dose-dependent manner which subsequently led to a dose-dependent decrease in MRI signal intensity. In addition, we explored the role of SPIO in inducing iDC autophagy and determined whether it assists in the uptake of the exogenous antigen ox-LDL into iDCs. Lastly, we investigated MR imaging is a feasible way to monitoring transplanted iDCs *in vivo*, and the mechanism through which SPIO labeling limits iDC vaccine efficacy.

Materials and methods

Ethics statement

All experiments were conducted as per the Guide for the Care and Use of Laboratory Animals published by

National Research Council. Further, the protocols for all animal experiments were approved by the Animal Care and Use Committee of Guangdong Province, China. All animals were cared for according to the guidelines developed by the China Council on Animal Care.

Nano-magnetic labeling materials

SPIO (carboxydextran-coated Fe_2O_3 , diam. = 80–150 nm) was provided by the Medical Imaging Center of Southern Medical University (Guangzhou, China). It was prepared from $\text{FeCl}_3 \cdot 6\text{H}_2\text{O}$, $\text{FeCl}_2 \cdot 4\text{H}_2\text{O}$ and dextran using a chemical co-precipitation process.

iDC preparation and SPIO labeling

Rabbit peripheral blood was filtered through a nylon mesh, and peripheral blood mononuclear cells (PBMCs) were isolated by Ficoll-Hypaque centrifugation. To obtain iDCs, PBMCs were cultured in RPMI-1640 (Life Technologies Inc., USA) supplemented with 50 U penicillin/ml and 50 mg streptomycin/l, hereafter referred to as “complete medium,” for 4 h at 37 °C and 5 % CO_2 . Then, the nonadherent cells were discarded, and the adherent cells were incubated in complete medium supplemented with 50 ng recombinant human granulocyte-macrophage colony-stimulating factor (GM-CSF)/ml and interleukin-4 (IL-4) (PeproTech, Rocky Hill, NJ, USA) for 7 days for further differentiation. On days 2 and 5, 75 % of the culture medium was replaced with fresh medium [complete medium supplemented with aspirin (dissolved in ethanol at 2.5 mM), GM-CSF, and IL-4]. On day 7, iDCs were harvested and incubated with different concentrations of SPIO in the presence of 1.5 μg poly-L-lysine/ml (PLL; Sigma) in a medium free of fetal bovine serum (FBS) for 24 h. The labeled-iDCs thus obtained were used for further experiments.

Identification of iDCs

To detect the expression of CD86 and HLA-DR on the cell surface, on day 7, 5×10^5 iDCs were harvested washed 3 times in PBS, and incubated with fluorescein isothiocyanate (FITC)- or R-phycoerythrin (PE)-labeled anti-CD86 or anti-HLA-DR (BD Co. Inc., Franklin Lakes, NJ) according to manufacturer's

instructions for 30 min at 4 °C in the dark. Subsequently, the cells were washed 3 times with precooled PBS and resuspended in PBS to perform flow cytometry analysis. All flow cytometry acquisition and analysis was performed on a flow cytometer (FACSCanto, BD Co. Inc.). Cell morphology was examined under a light microscope after Giemsa staining, which was carried out after 7 days on cells adherent to PLL-coated glass slides.

Magnetic resonance imaging

Varying numbers of cells were transferred after incubating with SPIO into 1.5 ml Eppendorf tubes loaded with 1 ml 1 % (w/v) agarose. Unlabeled cells of the same densities were processed in the same manner to serve as the negative control. MRI was performed on a 1.5 T instrument (GE Sigma HD 1.5 T MR) with a 12.7 cm receive-only knee coil. Samples were imaged using a gradient-echo T2* sequence (reception time [ms]/echo time [ms] = 620/15.7, 35° flip angle) with the section thickness of 2 mm and field view of 13 × 13 cm². Images were obtained with a matrix size of 256 × 256. The region of interest (ROI) for signal intensity (SI) measurement was 14.6 mm². Twelve ROIs were randomly selected. The percent change of SI (ΔSI) was calculated using the equation:

$$\Delta SI = (SI_l - SI_{ul})/SI_{ul} \times 100 \%,$$

where SI_l and SI_{ul} are the SI of the labeled cells and unlabeled cells, respectively.

MRI for the *in vivo* imaging of iDC migration to the liver was performed with knee coil on a 1.5T MRI with 3/0.5 mm slice thickness. iDCs labeled with 50 $\mu\text{g Fe/ml}$ SPIO were injected into the rabbits via the ear vein (5×10^5 cells/ml, 2 ml per rabbit) in the iDCs transplant group, and the same amount of physiological saline was injected into control group rabbits. After anesthesia and immobilization in the prostrate position, rabbits were scanned by magnetic resonance at 24 h after cells transplantation. MRI tracking was performed in fs T2WI sequence: TR = 5,500 ms; TE = 106.6 ms; FOV = 14.0 mm; and matrix size, 256 × 256.

Prussian blue staining

iDCs adhered to PLL-coated glass slides were fixed with 4 % (v/v) glutaraldehyde for 20 min, followed by

treatment with 2 % (w/v) potassium ferrocyanide/1.65 M HCl (1:1 v/v) for 20 min. Cells were washed 3 times with PBS. The percentage of iron-positive cells (blue) in approx. 300 cells was determined using light microscopy.

Atomic absorption spectrometry assay

Atomic absorption spectrometry was employed to detect intracellular iron to more accurately estimate labeling efficiency. A polarized Zeeman atomic absorption spectrometer (Hitachi, model Z-8200, Japan) was used for this. Iron measurements were performed at a 248.3 nm. The spectrometer was calibrated with six standards, containing iron from 89.55 to 3,582 μM in 0.05 HCl. For quality control, Lyphochek controls (Bio-Rad Laboratories, Munich, Germany) were used.

Cell viability assay

Because peripheral blood-derived iDCs are non-proliferative, the Cell Counting Kit-8 (CCK8; Dojindo Laboratories, Kumamoto, Japan) was used to examine cell viability. On day 7, DCs were harvested, and resuspended in a flat-bottomed 96-well plate at 10^5 cells per 100 μl media (free of FBS) in quintuplicate before SPIO labeling. The CCK8 assay was performed 24 h after SPIO labeling. The absorbance of each well was read in a plate reader at 450 nm. The absorbance value of the background spectra of the cell-free culture medium was deducted from each sample. The survival rate was calculated using the equation:

$$\text{Survival rate} = (\text{NonA}_{450} - \text{TreA}_{450})/\text{NonA}_{450} \times 100 \%,$$

where TreA_{450} was the absorbance value of SPIO-treated cells, and NonA_{450} was the absorbance value of non-SPIO-treated cells.

LysoTracker Red (LTR) staining

To explore the effect of SPIO labeling on lysosomal content in iDCs, LysoTracker Red DND-99 (Molecular Probes, Eugene, OR) was used to visualize lysosomes with a laser scanning microscopy combination system (LSM510/ConfoCor2; Zeiss, JENA, Germany). In brief, cells harvested on day 7 were washed with PBS and incubated for 2 h at 37 °C with 1 μM LTR in culture

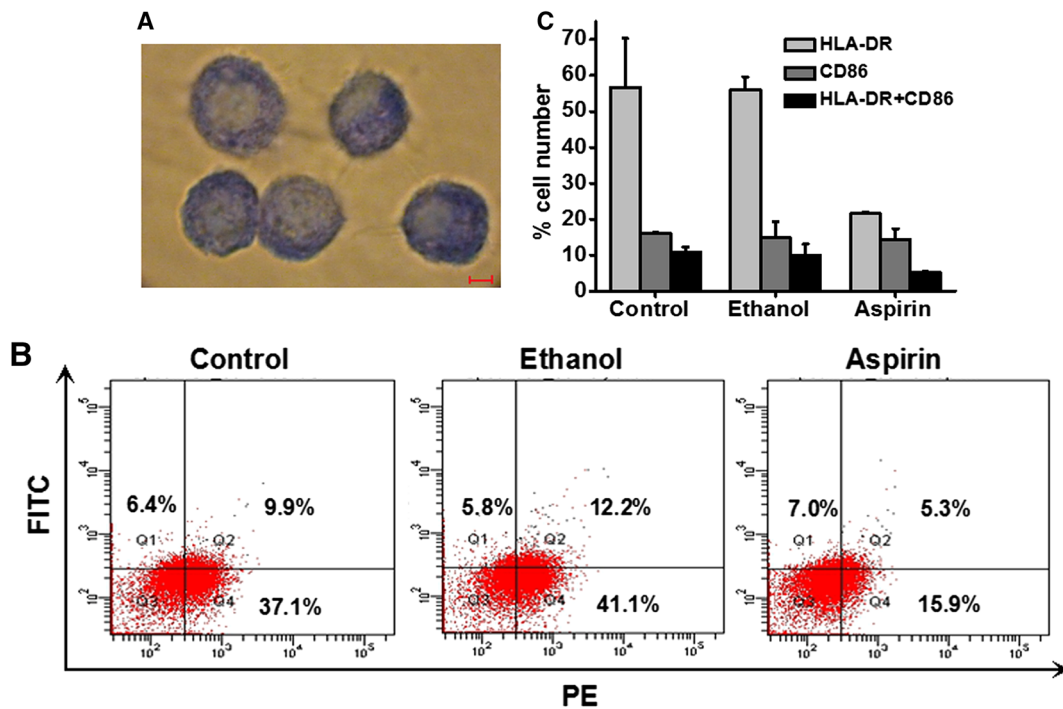


Fig. 1 Identification of iDCs. Peripheral blood-derived iDCs were generated as described in Materials and Methods, in the presence or absence of 2.5 mM aspirin and were harvested on day 7. **a** Giemsa staining. Aspirin-treated iDCs showed an immature phenotype with short, needle-like protrusions and a rounded nucleus. Flow cytometric analysis of the expression of

HLA-DR (PE) and CD86 (FITC) on iDCs. Cells cultured in the absence of aspirin were controls, and the maturation state of the cells, which were cultured in presence of ethanol, the solvent for aspirin, was also examined. Scale bars = 5 μ m. **b** The percentages of marker-positive cells (%), **c** in 3 different experiments are shown. Error bars represent the standard deviation

medium. After two washes with the culture medium, cells were resuspended in fresh culture medium and viewed immediately under a laser-scanning microscope. For the measurement, the excitation wavelength was 543 nm, and the emission-detection filter was BP 560–615 nm. To quantify cellular lysosomal mass, the images were processed with Zeiss Rel3.2 image processing software (Zeiss, JENA, Germany).

Transfection

Dendritic cells were transfected with the EGFP-LC3 plasmid containing a gene encoding enhanced-green fluorescent protein-tagged microtubule-associated protein 1 light chain 3 (a kind gift from Dr. Yoshimori) using Lipofectamine LTX and Plus reagents (Invitrogen, Paisley, U.K.). The transfected cells were treated with various concentrations of SPIO for 24 h before being examined with a laser scanning microscopy combination system for autophagosome assessment.

Analysis of ox-LDL uptake

To analyze its uptake by iDCs, oxidized low-density lipoprotein (ox-LDL) was labeled with 1,1'-dioctadecyl-3,3,3',3'-tetramethylindocarbocyanine perchlorate (DiI), a fluorescent dye. SPIO-labeled iDCs were incubated with DiI-conjugated ox-LDL (Yiyuan Biotechnologies., Guangzhou, China) for 4 h. Then, the cells were washed 3 times with culture media, and fluorescence was measured using a laser-scanning microscope. The excitation wavelength was 543 nm, and the emission detection filter was BP 560–615 nm. To quantify the results, the average fluorescence emission intensities of iDCs were processed with Zeiss Rel3.2 image processing software.

Intracellular localization of SPIO

Localization of SPIO in cells was analyzed by laser scanning microscopy using FITC (Sigma).

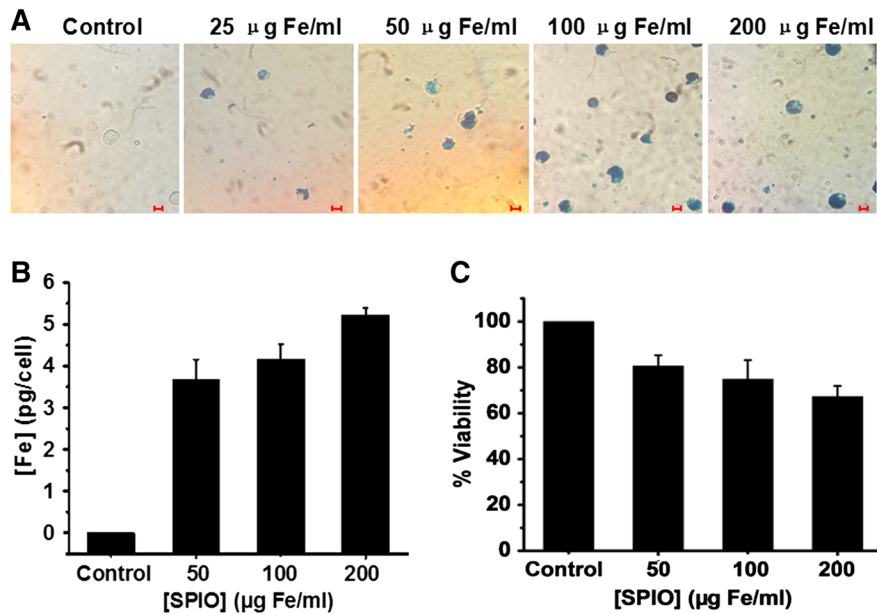


Fig. 2 SPIO-labeling of iDCs. At day 7 of iDC culture, SPIO was added to the cells in different concentrations ranging from 0 to 200 µg Fe/ml and the cells were cultured for 24 h. The cells were harvested and washed for further experiments. **a** Prussian blue staining of iDCs incubated with various concentrations of SPIO showing the iron distribution in cells $\times 400$. Scale

bars = 20 µm. **b** Cells were collected for atomic absorption spectrometry analysis, and iron content in each cell was calculated. **c** The viability of SPIO-iDCs was tested after prolonged culture using a CCK8 assay. *Graphs (b) and (c) show the mean of three independent experiments. Error bars represent the standard deviation*

Statistical analysis

Data are presented as mean \pm SD and were analyzed with Origin 7 (OriginLab Corporation) using two-sample *t*-test and one-way ANOVA analysis (Bonferroni correction). Differences with $*p < 0.05$ and $**p < 0.01$ were considered statistically significant.

Results

Aspirin can be used effectively to develop iDCs

To obtain iDCs *in vivo*, the cells were treated with aspirin from day 2 onward. Aspirin-treated dendritic cells not only exhibited typical dendritic morphology—nonadherent, rough cell surface, numerous wrinkles, and dendritic processes—but also displayed an immature phenotype, evidenced by a round nucleus and needle-like protrusions (Fig. 1a). To provide further molecular evidence, HLA-DR and CD86 expression on the cell surface was analyzed, because upregulation of these two molecules is indicative of

DC maturation. The expression of HLA-DR and CD86, especially HLA-DR, on the cell surface was lower in the aspirin-treated cells than in the controls (Fig. 1b, c).

SPIO labels iDCs with high efficiency, but exhibits dose-dependent cytotoxicity

To find the optimal concentration for SPIO labeling of iDCs, the efficiency of SPIO labeling, indicated by cell iron content, and the effect of SPIO labeling on cell viability were investigated. Prussian blue staining revealed the high efficiency of SPIO endocytosis by iDCs (Fig. 2a). The percentage of iron-containing cells and the intracellular iron content in each cell both increased with increasing label concentration. More precise values for the mean iron content in each individual cell was obtained by quantitative analysis of intracellular iron content by atomic absorption spectroscopy (Fig. 2b).

CCK8 assays revealed that cell viability decreased in a dose-dependent manner (Fig. 2c), and 50 µg Fe/ml SPIO was the optimal concentration for iDC iron

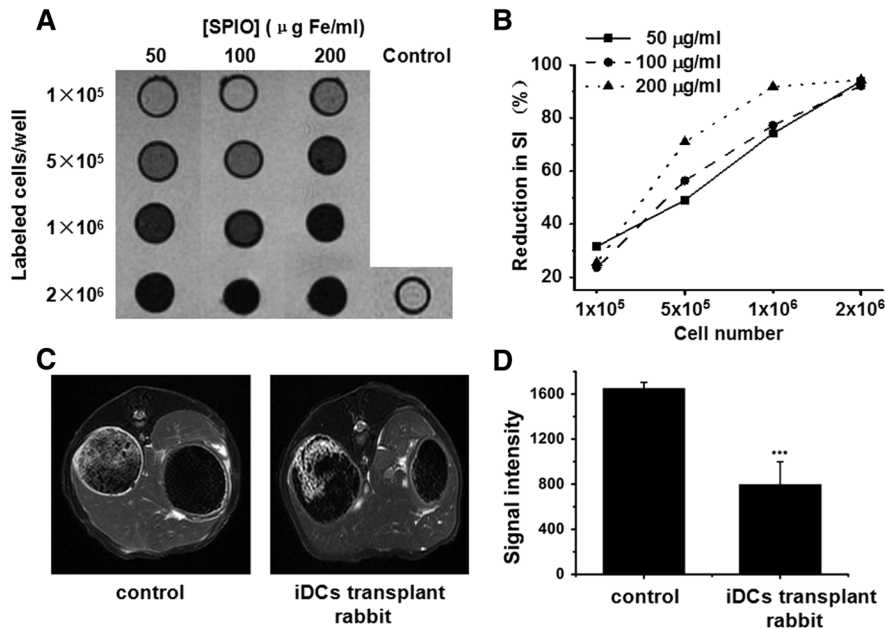


Fig. 3 In vitro and in vivo MRI. **a** Different numbers of cells in each condition were embedded in 1 ml of 1 % agarose and imaged on a 1.5 T MR system. Cells cultured in absence of SPIO were taken as controls. **b** Decrease in signal intensity (Δ SI) caused by SPIO labeling of iDCs at 1.5 T with a T2* acquisition. **c** MR images of rabbits before bolus injection of SPIO-labeled iDCs were taken as controls. MR images of

uptake, with >99 % of the cells containing iron at an average of 3 pg Fe/cell and minimal impact on cell viability.

MRI scanning in vitro and in vivo

To evaluate the effect of SPIO labeling on MRI, SPIO-iDCs (1×10^5 cells to 2×10^6 cells) were embedded in 1 ml of 1 % agarose, and the agar was imaged using a 1.5 T MR-scanner with a T2* acquisition, a sequence responsive to cell density change (Yang et al. 2012). As shown, SPIO-labeled iDCs were more hypointense than unlabeled iDCs, and the decrease in signal intensity was dependent on both the density of SPIO-iDCs and SPIO incubation concentration (Fig. 3a). For each sample, the Δ SI was calculated as described in Materials and Methods, and the data are shown in Fig. 3b. At 50 μ g Fe/ml SPIO, a distinguishable signal intensity decrease (about 50 %) was caused at 5×10^5 cells/cm³ at 1.5 T.

To measure the migration of SPIO-labeled iDCs, in vivo MRI scanning was performed. The MR signal

rabbits after bolus injection of SPIO-labeled iDCs were as assigned to iDC transplant rabbit groups. iDC transplant rabbits showed decreased signal intensity (lower luminance) in liver. **d** Quantification of the MRI signal intensity of 3 different slices within a region of interest within the rabbit liver. Error bars represent the standard deviation of 3 independent experiments. *** $p < 0.001$, compared to controls

intensity of tissues is more heterogeneous and higher than that of the in vitro test samples. We estimated that 5×10^5 cells/cm³ with 50 μ g Fe/ml SPIO can be detected with a 1.5 T whole body MR scanner in rabbits. Intravenous bolus injection of SPIO-labeled iDCs resulted in a strong signal loss in the liver tissue (Fig. 3c and d). The livers of iDC-transplant rabbits were darker than those of control group rabbits. In addition, the drop in signal intensity was by about 50 % more in the liver of iDC transplant rabbits than in the liver of control group rabbits. These findings suggest that transplanted iDCs labeled by SPIO can be dynamically tracked in vivo by MRI.

SPIO labeling induces autophagy in iDCs

The ability of SPIO to induce autophagy in iDCs was determined using LysoTracker Red, which labels acid compartments including autophagy vacuoles and lysosomes. Exposure of iDCs to SPIO for 24 h led to acidic lysosome/autophagosome production, which increased with the concentration of SPIO (0–200 μ g

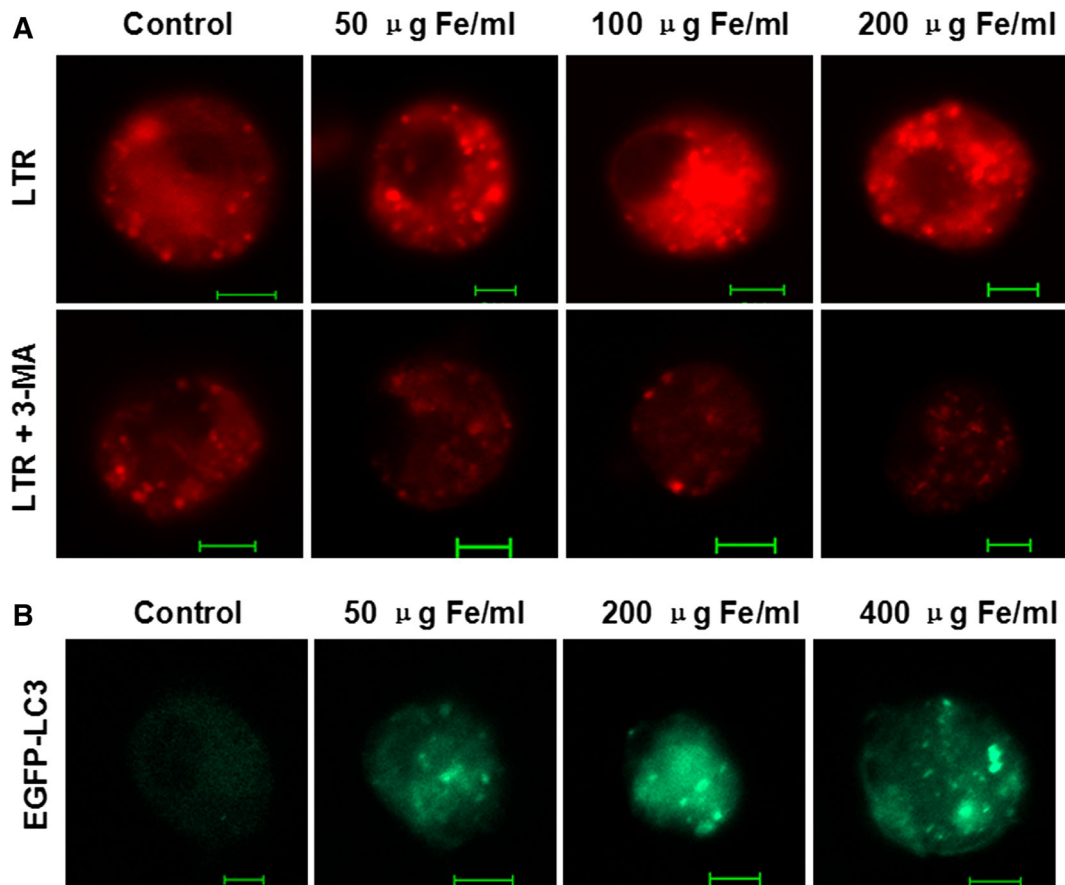


Fig. 4 Indication of autophagy in iDCs after different concentrations of SPIO labeling for 24 h. **a** *Red dots* represent lysosomes in iDCs, SPIO labeling induced increased autophagy lysosome formation in iDCs, and the increase was abrogated when 3-MA, an autophagy inhibitor, was added. **b** SPIO induced

LC3 puncta formation in iDCs. *Green dots* represent autophagosomes. Typical photograph of transfected cells treated with 0, 50, 200, or 400 µg Fe/ml SPIO for 24 h is shown Scale bars = 5 µm

Fe/ml) (Fig. 4a). The lower panel in Fig. 4a shows that the increase was inhibited by 3-methyladenine, a widely used autophagy inhibitor, strongly suggesting that the increase was due to production of autophagy lysosome in the cell. To study the autophagy induction in iDCs further, the plasmid EGFP-LC3 was transfected into iDCs to mark the occurrence of autophagy (Fig. 4b). The protein LC3 specifically associates with autophagosome membranes. The results suggested that exposure to SPIO at 50, 200, and 400 µg Fe/ml induced EGFP-LC3 dot generation in iDCs in a dose-dependent manner. Taken together, these results suggest that SPIO labeling induces autophagosome formation in iDCs.

SPIO-labeled iDCs possess lower antigen phagocytosis capacity than non-labeled iDCs

Because SPIO induces autophagy, which is thought to be a facilitator of endogenous antigen processing in iDCs, it might also affect the exogenous antigen processing ability of iDCs. To explore the effect of SPIO labeling on the antigen phagocytic capacity of iDCs, SPIO-labeled cells were examined by laser scanning microscopy for intracellular fluorescence after incubating with DiI-ox-LDL for 4 h. The mean fluorescence intensity of 200 cells for each condition was calculated. As shown in Fig. 5a and b, ox-LDL uptake was higher in unprocessed iDCs than in

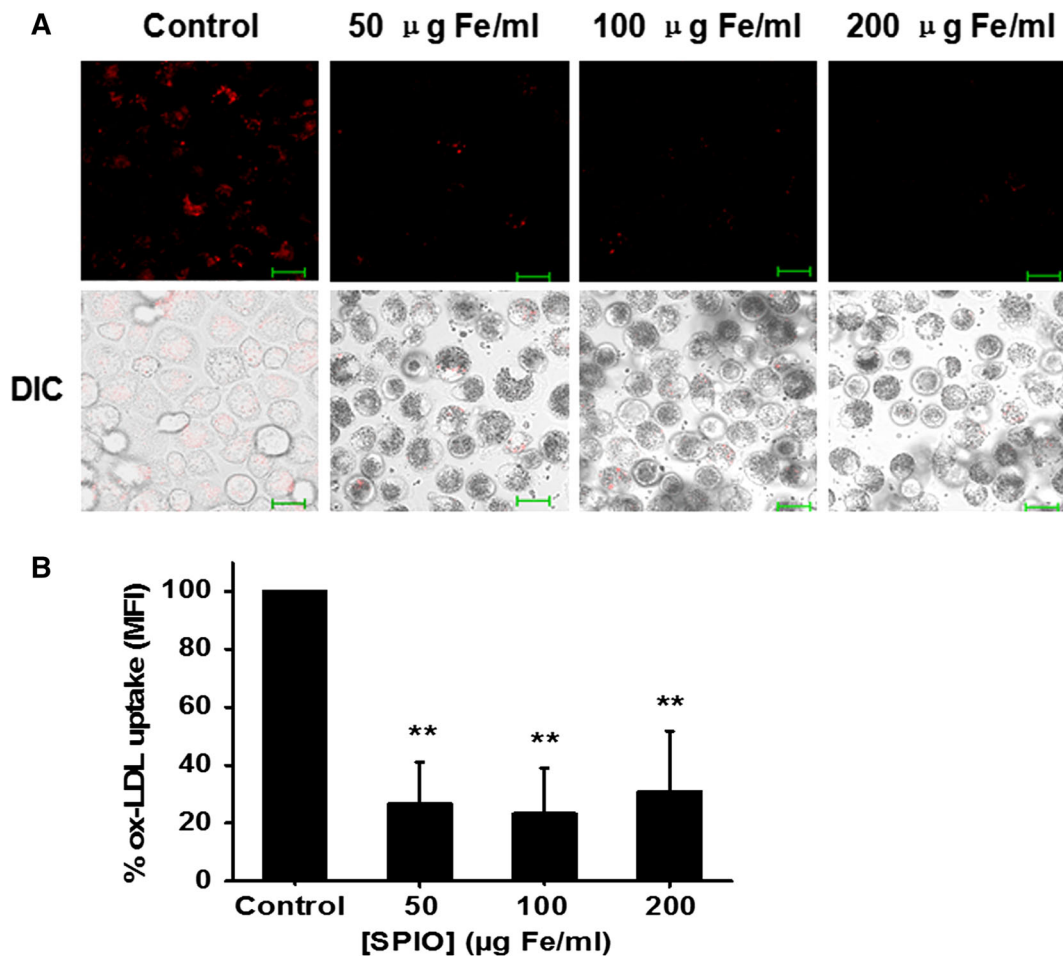


Fig. 5 Uptake of DiI-ox-LDL by SPIO-treated dendritic cells. **a** Fluorescence images of iDCs that were treated with DiI-ox-LDL for 4 h. Representative photomicrographs from 3 independent experiments are shown. Scale bars = 20 µm. **b** Mean fluorescence intensity of the DiI-treated cells under different

conditions. Fluorescence intensity of the control group, which comprised cells cultured without SPIO, was set as 100 %. For each sample, about 200 cells were used for the calculation. *Error bars* represent the standard deviation of 3 independent experiments. ** $p < 0.01$, compared to controls

processed iDCs. After treatment with SPIO, the percentage of ox-LDL-containing cells and the amount of ox-LDL in each individual cell were both decreased. SPIO labeling decreased the phagocytic capacity of the cells by 70–80 %, and there was no significant difference between the treatment groups.

Internalized SPIO and ox-LDL are both directed to lysosomes

Because the phagocytosed antigens are first directed to lysosomes to be degraded into smaller fragments and to be presented, we hypothesized that the decreased antigen phagocytosis capacity of iDCs could be the

result of lysosomes being occupied by the engulfed SPIO, which would then hamper the processing of other engulfed antigens. To verify this hypothesis, the subcellular localizations of SPIO and ox-LDL were analyzed by laser scanning microscopy with FITC and DiI labeling. The results showed that SPIO and ox-LDL colocalized to the lysosomes (Fig. 6a, b).

Discussion

In our study, although the sensitivity of MRI detection of cells increased with the increase in SPIO concentration used in the co-culture, cell viability decreased

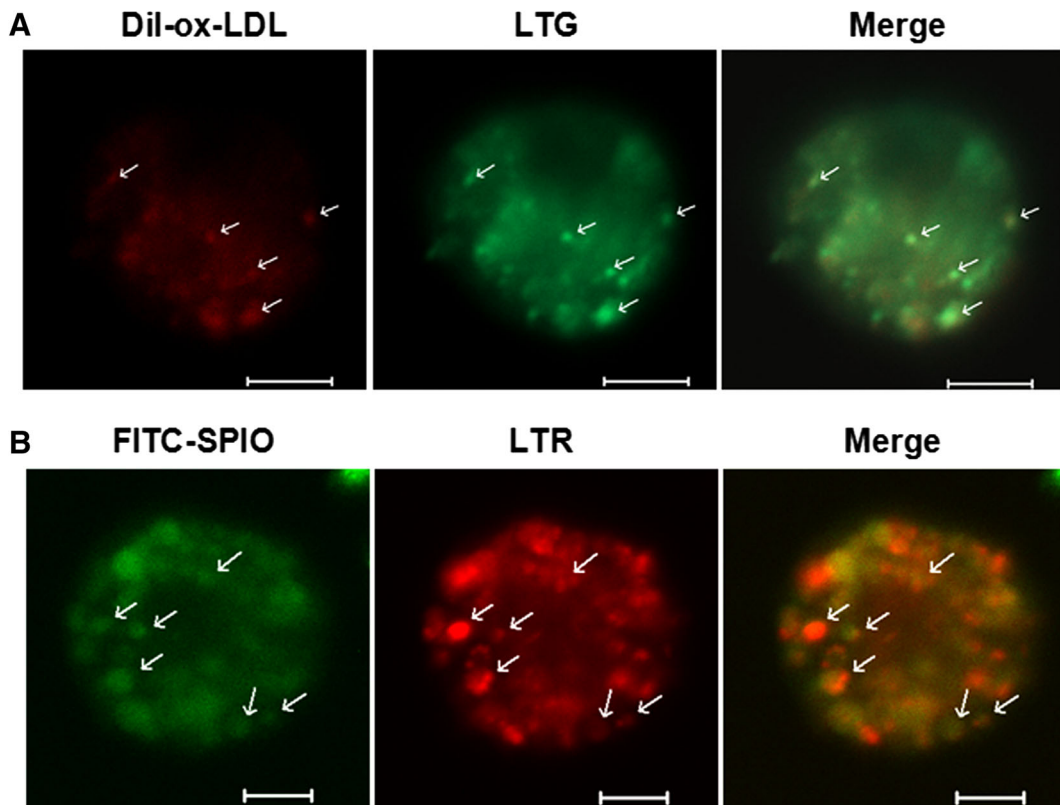


Fig. 6 Localization of internalized SPIO and ox-LDL to the lysosomes. **a** The cells were cultured for 7 days without SPIO treatment, and then harvested and treated with DiI-ox-LDL and LTG (LysoTracker Green) for 4 and 2 h, successively. Cellular localization of both molecules was observed by confocal

microscopy. **b** Cells at day 7 were treated for 24 h with SPIO (100 $\mu\text{g Fe/ml}$) labeled with the *green* dye FITC, and then treated with LTR for another 2 h. Confocal microscopy was used to show the distribution of the two fluorescent dyes. Scale bars = 5 μm

with increasing SPIO concentration. Incubation of iDCs with 50 $\mu\text{g Fe/ml}$ SPIO resulted in considerable signal change in MRI, with cell viability being affected only slightly. On the basis of previous reports on cell transplantation and in vivo imaging, we concluded that 5×10^5 cells/ cm^3 with 4 pg Fe/cell (co-cultured with 50 $\mu\text{g Fe/ml}$ SPIO) can be detected with a 1.5 T whole body MR scanner in rabbits.

Autophagy is a life-sustaining process whereby cytoplasmic components and damaged organelles are sequestered in double-membrane vesicles called autophagosomes and are degraded upon fusion of the autophagosomes with lysosomes. A variety of inorganic and organic nanomaterials have been reported to cause varying degrees of autophagy, such as nano-neodymium oxide, fullerene C60, and cationic liposomes (Man et al. 2010; Zhang et al. 2009). As a nanomaterial, SPIO may also exert this effect. Iron

oxide nanoparticles can cause autophagy in A549 cell, but not in normal cells (Khan et al. 2012). We investigated whether SPIO would cause autophagy in iDCs. Our findings demonstrated that autophagy was indeed induced in cells treated with SPIO, especially in cells treated with high concentrations of SPIO, for 24 h. These observations suggest that the internalized SPIO may be degraded, at least in part, via the autophagy pathway.

As an important antigen-presenting cell (APC) with a central role in controlling immunity, iDCs need to possess excellent antigen uptake ability. It is therefore necessary to know whether SPIO labeling influences iDC uptake ability. Baumjohann et al. (2006) found that the capacity of labeled DCs to prime syngeneic T cells was slightly decreased. However, the cause of the decrease in antigen uptake or antigen processing was not clarified. In this study, ox-LDL, an atherosclerosis

antigen, was used to assess the effect of SPIO labeling on the antigen uptake ability of iDCs. Labeling indeed decreased the antigen phagocytic capacity of iDCs. Our observations suggest that both SPIO and ox-LDL are directed to lysosomes for further degradation. Therefore, we propose that the engulfed SPIO occupied more lysosome space than it induced in cells, thereby hindering the phagocytosis of ox-LDL.

Conclusion

we reveal here that MRI (fs T2WI sequence) can efficiently track SPIO-labeled iDCs and could be a feasible method for monitoring transplanted iDCs in vivo. SPIO effectively labeled iDCs, but caused some degree of damage to the cells. High SPIO concentrations induced autophagy. SPIO labeling significantly impaired the antigen phagocytic capacity of iDCs. This was likely caused by the occupation of lysosomes by the internalized SPIO. It is the first step to determining the optimal SPIO loading concentration for effective cell labeling without damaging cells. Future studies should focus on the effect of SPIO on surface molecule expression, maturity status, and antigen presentation of iDCs to confirm whether SPIO will influence their immunosuppressive ability.

Acknowledgments This study was supported by the National Natural Science Foundation of China (81471659 and 31170250). We are grateful to Dr. Yoshimori (Laboratory of Genetics Graduate School of Medicine, Osaka University) for kindly providing the plasmid EGFP-LC3. SPIO was provided by Professor Xu Yikai (Department of Medical Imaging Center, Nan Fang Hospital, Southern Medical University, No. 1838 Guangzhou Avenue North, Guangzhou, Guangdong, 510515, China).

References

Baumjohann D, Hess A, Budinsky L, Brune K, Schuler G, Lutz MB (2006) In vivo magnetic resonance imaging of

- dendritic cell migration into the draining lymph nodes of mice. *Eur J Immunol* 36:2544–2555
- Datta A, Raymond KN (2009) Gd—hydroxyypyridinon (HOPO)-based high-relaxivity magnetic resonance imaging (MRI) contrast agents. *Acc Chem Res* 42:938–947
- Jagannath C, Lindsey DR, Dhandayuthapani S, Xu Y, Hunter RL Jr, Eissa NT (2009) Autophagy enhances the efficacy of BCG vaccine by increasing peptide presentation in mouse dendritic cells. *Nat Med* 15:267–276
- Khan MI, Mohammad A, Patil G, Naqvi SA, Chauhan LK, Ahmad I (2012) Induction of ROS, mitochondrial damage and autophagy in lung epithelial cancer cells by iron oxide nanoparticles. *Biomaterials* 33:1477–1488
- Klotz L, Dani I, Edenhofer F, Nolden L, Evert B, Paul B, Kolanus W, Klockgether T, Knolle P, Diehl L (2007) Peroxisome proliferator-activated receptor gamma control of dendritic cell function contributes to development of CD4 + T cell anergy. *J Immunol* 178:2122–2131
- Lunov O, Syrovets T, Röcker C, Tron K, Nienhaus GU, Rasche V, Mailänder V, Landfester K, Simmet T (2010) Lysosomal degradation of the carboxydextran shell of coated superparamagnetic iron oxide nanoparticles and the fate of professional phagocytes. *Biomaterials* 31:9015–9022
- Man N, Chen Y, Zheng F, Zhou W, Wen LP (2010) Induction of genuine autophagy by cationic lipids in mammalian cells. *Autophagy* 6:449–454
- Paludan C, Schmid D, Landthaler M, Vockerodt M, Kube D, Tuschl T, Münz C (2005) Endogenous MHC class II processing of a viral nuclear antigen after autophagy. *Science* 307:593–596
- Tavaré R, Sagoo P, Varama G, Tanriver Y, Warely A, Diebold SS, Southworth R, Schaeffter T, Lechler RI, Razavi R, Lombardi G, Mullen GED (2011) Monitoring of in vivo function of superparamagnetic iron oxide labeled murine dendritic cells during anti-tumour vaccination. *PLoS ONE* 6:e19662
- Yang FY, Yu MX, Chen WL, Zhou Q, Gao P, Huang Z (2012) Effects of iron oxide nanoparticle labeling on human endothelials. *Cell Transplant* 21:1805–1820
- Zabimyk O, Yezhelyev M, Seleverstov O (2007) Nanoparticles as a novel class of autophagy activators. *Autophagy* 3:278–281
- Zhang Q, Yang W, Man N, Zheng F, Shen Y, Sun K, Li Y, Wen LP (2009) Autophagy-mediated chemosensitization in cancer cells by fullerene C60 nanocrystal. *Autophagy* 5:1107–1117
- Zhou J, Yang FY, Zhou Q, Yang KR, Chen WL (2014) Magnetic resonance imaging tracking of ultra small superparamagnetic iron oxide labeled rabbit dendritic cells. *Exp Biol Med* 239:13–23